

## Effect of multiplicative noise on stationary stochastic process

A. V. Kargovsky,\* A. Yu. Chikishev, and O. A. Chichigina

*Faculty of Physics and International Laser Center, Lomonosov Moscow State University, Leninskie Gory, 119991 Moscow, Russia*



(Received 29 July 2017; published 14 March 2018)

An open system that can be analyzed using the Langevin equation with multiplicative noise is considered. The stationary state of the system results from a balance of deterministic damping and random pumping simulated as noise with controlled periodicity. The dependence of statistical moments of the variable that characterizes the system on parameters of the problem is studied. A nontrivial decrease in the mean value of the main variable with an increase in noise stochasticity is revealed. Applications of the results in several physical, chemical, biological, and technical problems of natural and humanitarian sciences are discussed.

DOI: [10.1103/PhysRevE.97.032112](https://doi.org/10.1103/PhysRevE.97.032112)

### I. INTRODUCTION

There has been considerable recent interest in the statistical analysis of systems in the presence of specific random forces. The stochastic nature of such systems and related noise-induced effects are important for stochastic thermodynamics [1–4], nanotechnology [5–7], electronics [8–11], ornithology [12–17], population dynamics [18–21], epidemiology [22–26], and the study of cultural heritage [27]. Experimental and computational results show similarities in the behavior of these systems.

Most works consider Gaussian white noise. However, more general and realistic models of noise source are necessary. Thus, different types of pulse noise have been used to model random processes. There has been considerable recent interest in the role of multiplicative quasiperiodic noise in systems at steady state [9,28,29].

In conventional scenarios of statistical physics, the loss of energy results from thermal fluctuations, while energy input is deterministic in an equilibrium state. We will show that alternative models with random input of energy and deterministic dissipation can also be used to describe real processes. If a random external accelerating force is significant, thermal fluctuations can be neglected.

In this work, we analyze the effect of random quasiperiodic pulse pumping on a stationary-state system with nonlinear dissipation. The dynamics of the main variable that characterizes the system is described using a stochastic differential equation that allows generalization of the earlier results. The tasks are as follows: (i) Derivation of analytical expressions for the probability distribution and moments and analysis of the expressions with allowance for variations in parameters. (ii) Numerical simulation aimed at an application of the expressions in the analysis of processes with pulse noise with controlled periodicity. (iii) A search for parameters for which analytical expressions for statistical moments can be derived in the presence of an arbitrary noise. (iv) Analysis of

possible applications in several physical, chemical, biological, and technical problems of natural and humanitarian sciences.

### II. ANALYTICAL STUDY

We consider the Langevin equation with multiplicative noise for a random non-negative quantity  $x$ :

$$\frac{dx}{dt} = -bx^\beta + x^\gamma \eta(t), \quad (1)$$

where  $b > 0$  is the damping factor,  $\eta(t)$  is the stationary random process with positive mean value  $\langle \eta(t) \rangle = a$ , and the exponents satisfy the following inequalities:  $0 \leq \gamma < 1$  and  $\beta > \gamma$ . We consider noise sources for which the main statistical characteristics are determined to be finite (for other cases, see, for example, Ref. [30]).

#### A. Fokker-Planck equation

First, the system with the Gaussian white noise is studied. Extracting the mean value of the noise component, we represent Eq. (1) as

$$\frac{dx}{dt} = ax^\gamma - bx^\beta + x^\gamma \xi(t), \quad (2)$$

where  $x \in \mathbb{R}^+$ , and  $\xi(t)$  is the Gaussian white noise with  $\langle \xi(t) \rangle = 0$  and  $\langle \xi(t)\xi(t') \rangle = 2D\delta(t-t')$ . Here, we use the Stratonovich interpretation of SDE's [8].

Introducing a new variable  $z = \frac{x^{1-\gamma}}{1-\gamma}$ , we reduce Eq. (2) to

$$\frac{dz}{dt} = a - b[(1-\gamma)z]^{\frac{\beta-\gamma}{1-\gamma}} + \xi(t). \quad (2')$$

The corresponding Fokker-Planck equation for the probability density function  $w(z,t)$  is

$$\frac{\partial w}{\partial t} = D \frac{\partial^2 w}{\partial z^2} - \frac{\partial}{\partial z} [(a - b[(1-\gamma)z]^{\frac{\beta-\gamma}{1-\gamma}})w]. \quad (3)$$

\*kargovsky@yumr.phys.msu.ru

The stationary solution to Eq. (3) can be represented as

$$w_{st}(z) = \mathcal{N} e^{\frac{az}{D} - \frac{b}{D\lambda}(1-\gamma)^{\lambda-1} z^\lambda}, \quad (4)$$

where  $\lambda = \frac{\beta-\gamma}{1-\gamma} + 1$  and  $\mathcal{N}$  is the normalization constant.

Using integral  $\mathcal{I}_0$  from Appendix A, we derive the following expression in terms of the variable  $x$ :

$$w_{st}(x) = \lambda(1-\gamma) \left(\frac{b}{D\lambda(1-\gamma)}\right)^{\frac{1}{\lambda}} x^{-\gamma} \frac{e^{\frac{a}{D(1-\gamma)}x^{1-\gamma} - \frac{b}{D\lambda(1-\gamma)}x^\lambda(1-\gamma)}}{{}_1\Psi_0\left(\frac{1}{\lambda}, \frac{1}{\lambda} \middle| \kappa_D\right)}, \quad (5)$$

where  ${}_p\Psi_q(\dots|z)$  is the generalized hypergeometric Wright function [31]. Here we use the following notation for brevity:

$$\kappa_D = \frac{a}{D(1-\gamma)} \left(\frac{b}{D\lambda(1-\gamma)}\right)^{-\frac{1}{\lambda}}.$$

Then, the stationary moments of  $x$  are

$$\mu_n = \left(\frac{b}{D\lambda(1-\gamma)}\right)^{-\frac{n}{\lambda(1-\gamma)}} \frac{{}_1\Psi_0\left(\frac{1}{\lambda} + \frac{n}{\lambda(1-\gamma)}, \frac{1}{\lambda} \middle| \kappa_D\right)}{{}_1\Psi_0\left(\frac{1}{\lambda}, \frac{1}{\lambda} \middle| \kappa_D\right)}. \quad (6)$$

The results of [32] show that the Wright function can be reduced to a finite sum of generalized hypergeometric functions [33] when  $\lambda \in \mathbb{Q}$ .

Using integral  $\mathcal{I}(\omega)$  from Appendix B, we obtain the characteristic function of  $x$ ,

$$\Theta(\omega) = \frac{H_{1,0,0,1;0,1,0}^{0,1;1,0;1,0}\left(\left(1 - \frac{1}{\lambda}; \frac{1}{\lambda}, \frac{1}{\lambda(1-\gamma)}\right) : \text{---}; \text{---} \middle| -\kappa_D\right)}{{}_1\Psi_0\left(\frac{1}{\lambda}, \frac{1}{\lambda} \middle| \kappa_D\right)} \frac{-i\omega\left(\frac{b}{D\lambda(1-\gamma)}\right)^{-\frac{1}{\lambda(1-\gamma)}}}{-i\omega\left(\frac{b}{D\lambda(1-\gamma)}\right)^{-\frac{1}{\lambda(1-\gamma)}}}, \quad (7)$$

where  $H_{p,q;\dots}^{0,n;\dots}\left(\dots \middle| \begin{smallmatrix} z_1 \\ z_2 \end{smallmatrix}\right)$  is the generalized hypergeometric  $H$ -function of two variables [34].

When  $\beta = 1$ , the Wright function is reduced to the parabolic cylinder function [33,35], and we obtain the probability density function

$$w_{st}(x) = \sqrt{\frac{2b(1-\gamma)}{\pi D}} x^{-\gamma} \frac{e^{-\frac{b}{2D(1-\gamma)}(x^{1-\gamma} - \frac{a}{b})^2}}{\operatorname{erfc}\left(-\frac{a}{\sqrt{2bD(1-\gamma)}}\right)} \quad (8)$$

and the moments

$$\mu_n = \sqrt{\frac{2}{\pi}} e^{-\frac{a^2}{4bD(1-\gamma)}} \left(\frac{b}{D(1-\gamma)}\right)^{-\frac{n}{2-2\gamma}} \times \Gamma\left(\frac{n}{1-\gamma} + 1\right) \frac{D^{-\frac{n}{1-\gamma}} - 1\left(-\frac{a}{\sqrt{bD(1-\gamma)}}\right)}{\operatorname{erfc}\left(-\frac{a}{\sqrt{2bD(1-\gamma)}}\right)}, \quad (9)$$

which coincide with stationary results from [19,29].

It is of interest to determine parameter  $\mu_n$  in the limiting cases  $\kappa_D \rightarrow 0$  and  $\kappa_D \rightarrow \infty$ . As  $\kappa_D$  decreases with increasing parameter  $D$ , the limits correspond to high and low stochasticity, respectively. For small values of argument  $\kappa_D$ , we get

$$\mu_n = \left(\frac{b}{D\lambda(1-\gamma)}\right)^{-\frac{n}{\lambda(1-\gamma)}} \frac{\Gamma\left(\frac{1}{\lambda} + \frac{n}{\lambda(1-\gamma)}\right)}{\Gamma\left(\frac{1}{\lambda}\right)} \times \left\{ 1 + \left[ \frac{\Gamma\left(\frac{2}{\lambda} + \frac{n}{\lambda(1-\gamma)}\right)}{\Gamma\left(\frac{1}{\lambda} + \frac{n}{\lambda(1-\gamma)}\right)} - \frac{\Gamma\left(\frac{2}{\lambda}\right)}{\Gamma\left(\frac{1}{\lambda}\right)} \right] \kappa_D + O(\kappa_D^2) \right\}. \quad (10)$$

Using the asymptotic expansion of the Wright function for large values of the argument [36], we obtain for  $\kappa_D \rightarrow \infty$

$$\mu_n = \left(\frac{a}{b}\right)^{\frac{n}{\beta-\gamma}} \left\{ 1 + \frac{nD}{2} \frac{\gamma + n - \beta}{\beta - \gamma} \left[\frac{b^\frac{1}{\lambda}}{a}\right]^{\frac{1}{1-\lambda}} + O\left(D^2 \left[\frac{b^\frac{1}{\lambda}}{a}\right]^{\frac{2}{1-\lambda}}\right) \right\}. \quad (11)$$

Let us focus on the dependence of the mean value  $\langle x \rangle$  on parameter  $D$ . When  $\kappa_D \rightarrow 0$ ,  $\langle x \rangle$  tends to

$$\langle x \rangle = \left(\frac{b}{D\lambda(1-\gamma)}\right)^{-\frac{1}{\lambda(1-\gamma)}} \frac{\Gamma\left(\frac{1}{\lambda} + \frac{1}{\lambda(1-\gamma)}\right)}{\Gamma\left(\frac{1}{\lambda}\right)} \times \left\{ 1 + \left[ \frac{\Gamma\left(\frac{2}{\lambda} + \frac{1}{\lambda(1-\gamma)}\right)}{\Gamma\left(\frac{1}{\lambda} + \frac{1}{\lambda(1-\gamma)}\right)} - \frac{\Gamma\left(\frac{2}{\lambda}\right)}{\Gamma\left(\frac{1}{\lambda}\right)} \right] \kappa_D \right\}. \quad (12)$$

And for  $\kappa_D \rightarrow \infty$ , we have

$$\langle x \rangle = \left(\frac{a}{b}\right)^{\frac{1}{\beta-\gamma}} \left\{ 1 + \frac{D}{2} \frac{\gamma + 1 - \beta}{\beta - \gamma} \left[\frac{b^\frac{1}{\lambda}}{a}\right]^{\frac{1}{1-\lambda}} \right\}. \quad (13)$$

It is seen that, in this case, the mean value  $\langle x \rangle$  depends linearly on parameter  $D$ . For  $\beta = \gamma + 1$ , the mean value is almost independent of noise intensity.

In general, simple algebraic manipulations yield the following independence condition:

$$\left[ {}_1\Psi_0\left(\frac{2}{\lambda} + \frac{1}{\lambda(1-\gamma)}, \frac{1}{\lambda} \middle| \kappa_D\right) {}_1\Psi_0\left(\frac{1}{\lambda}, \frac{1}{\lambda} \middle| \kappa_D\right) - {}_1\Psi_0\left(\frac{1}{\lambda} + \frac{1}{\lambda(1-\gamma)}, \frac{1}{\lambda} \middle| \kappa_D\right) {}_1\Psi_0\left(\frac{2}{\lambda}, \frac{1}{\lambda} \middle| \kappa_D\right) \right] (1-\lambda) \times (1-\gamma)\kappa_D + {}_1\Psi_0\left(\frac{1}{\lambda} + \frac{1}{\lambda(1-\gamma)}, \frac{1}{\lambda} \middle| \kappa_D\right) \times {}_1\Psi_0\left(\frac{1}{\lambda}, \frac{1}{\lambda} \middle| \kappa_D\right) = 0. \quad (14)$$

Based on Eqs. (12) and (13) and the continuity of function  $\langle x \rangle(D)$ , we conclude that this function has at least one minimum for  $\beta > \gamma + 1$ .

Finally, the asymptotic expression for the variance is written as

$$\sigma_x^2 = \left(\frac{a}{b}\right)^{\frac{2}{\beta-\gamma}} \left\{ \frac{D}{\beta-\gamma} \left[ \frac{b^{\frac{1}{\lambda}}}{a} \right]^{\frac{1}{1-\frac{1}{\lambda}}} + O\left( D^2 \left[ \frac{b^{\frac{1}{\lambda}}}{a} \right]^{\frac{2}{1-\frac{1}{\lambda}}} \right) \right\}. \quad (15)$$

### B. Statistical moments for arbitrary noise

Several moments of  $x$  can be derived for a more general noise model in comparison with the model of the white Gaussian noise. We consider the random process  $\eta(t)$  that is characterized by spectral density  $S_\eta(\omega)$ . The main parameters of noise are the mean value  $a = \langle \eta(t) \rangle$  and the stochasticity (also called the intensity coefficient [8]), or the integral of correlation function,

$$D = S_{\eta-\langle \eta \rangle}(0)/4. \quad (16)$$

#### 1. Ergodic process with relatively low stochasticity

If  $\eta(t)$  is ergodic, process  $x$  can be considered ergodic at a stationary state. We divide Eq. (1) by  $x^\gamma$  and integrate starting from time  $t_s$ , when the system is already at a stationary state,

$$\frac{\Delta x^{1-\gamma}}{1-\gamma} = -b \int_{t_s}^t x^{\beta-\gamma} dt' + \int_{t_s}^t \eta(t') dt'. \quad (17)$$

For an ergodic process, the integrals on the right-hand side can be changed by mean values,

$$-b \int_{t_s}^t x^{\beta-\gamma} dt' + \int_{t_s}^t \eta(t') dt' = -b \Delta t \langle x^{\beta-\gamma} \rangle + a \Delta t. \quad (18)$$

We can neglect the fluctuating value  $\Delta x^{1-\gamma}$  on the left-hand side of Eq. (17) in comparison with the increasing right-hand side at a long time interval  $\Delta t$ .

Then, we get

$$\langle x^{\beta-\gamma} \rangle = \frac{a}{b}. \quad (19)$$

This moment is independent of noise stochasticity  $D$ . The same result comes from Eq. (11) up to terms of  $O(D^2 [b^{1/\lambda}/a]^{2\lambda/(\lambda-1)})$ .

#### 2. Noise with finite correlation time

We consider the system with a relatively large damping factor  $b$  and noise with finite correlation time  $\tau_c$ . Such a process corresponds to the limit  $\kappa_D \rightarrow 0$ . Below in this subsection, we integrate over such an interval  $\Delta t \gg \tau_c$  that

$$\left| \int_{t_s}^t \langle \xi(t) \xi(t') \rangle dt' - D \right| \ll D. \quad (20)$$

Parameter  $b^{-1}$  characterizes the relaxation time of the system. Assume that such a relaxation time is shorter than time  $\tau_c$ . Therefore, the correlation time of the process  $x(t)$  is shorter than  $\tau_c$ . Thus, quantity  $x^\alpha$  at arbitrary  $\alpha$  can also be averaged as

$$\left| \int_{t_s}^t (x^\alpha - \langle x^\alpha \rangle) dt' \right| \ll \langle x^\alpha \rangle \Delta t. \quad (21)$$

Multiplying Eq. (2') by  $z = \frac{x^{1-\gamma}}{1-\gamma}$ , we obtain

$$\frac{1}{2} \frac{dz^2}{dt} = az - b(1-\gamma)^{\frac{\beta-\gamma}{1-\gamma}} z^\lambda + z\xi(t). \quad (22)$$

Averaging of Eq. (22) at a stationary state yields

$$0 = a\langle z \rangle - b(1-\gamma)^{\frac{\beta-\gamma}{1-\gamma}} \langle z^\lambda \rangle + \langle z\xi(t) \rangle. \quad (23)$$

To estimate the third term in Eq. (23), we employ Eq. (2'):

$$\Delta z = a\Delta t - b \int_{t_s}^t [(1-\gamma)z]^{\frac{\beta-\gamma}{1-\gamma}} dt' + \int_{t_s}^t \xi(t') dt'. \quad (24)$$

In accordance with Eq. (21), we present integration as averaging in Eq. (17). In this case, noise fluctuations cannot be neglected,

$$\Delta z = a\Delta t - b \langle [(1-\gamma)z]^{\frac{\beta-\gamma}{1-\gamma}} \rangle \Delta t + \int_{t_s}^t \xi(t') dt'. \quad (25)$$

When Eq. (25) is substituted in correlator  $\langle z\xi(t) \rangle$ , the first and second terms vanish due to multiplication by  $\langle \xi(t) \rangle = 0$ . Thus, we have

$$\langle z\xi(t) \rangle = \left\langle \int_{t_s}^t \xi(t) \xi(t') dt' \right\rangle = D. \quad (26)$$

For Gaussian white noise, the result is obtained in [37].

For a stationary process, we obtain the following relation:

$$\langle x^{\beta+1-2\gamma} \rangle = (1-\gamma) \frac{D}{b} + \frac{a}{b} \langle x^{1-\gamma} \rangle. \quad (27)$$

The same result comes from Eq. (10) at  $n = \beta + 1 - 2\gamma$  and  $\kappa_D \rightarrow 0$ .

## III. NUMERICAL ANALYSIS

### A. Pulse noise

In Sec. II A, we consider white Gaussian noise. However, for numerous applications, pulse noise is more convenient. We assume that the stochastic process  $\eta(t)$  consists of  $\delta$  pulses with constant positive amplitude  $f_0$ , which is convenient for both analytical and numerical study,

$$\eta(t) = f_0 \sum_i \delta(t - t_i). \quad (28)$$

The parameters of such a noise source are determined by the statistics of time intervals between pulses. The interval between neighboring pulses is  $\tau_i = t_i - t_{i-1}$ . This random quantity has a mean value that coincides with the quasiperiod of the process, i.e.,  $\langle \tau \rangle = T$ .

We consider two different types of noise sources in Eq. (1). The first is the dead-time-distorted Poisson pulse (DTDP) process [38], and the second is the pulse process with fixed time intervals (FTIs) [9].

#### 1. Dead-time-distorted Poisson pulse noise

The DTDP process is a renewal pulse process with statistically independent and identically distributed intervals  $\tau$ . There is a dead-time interval  $\tau_0$  after each pulse. The arrival of the next pulse is forbidden over a dead-time interval. After the end of the interval, the probability per unit time of the next

pulse ( $p$ ) is constant. This process can be used to describe noise sources with varying degree of randomness, ranging from Poisson white noise ( $\tau_0 = 0$ ) to the quasiperiodic process ( $\tau_0 \lesssim T$ ) [20,28].

The probability distribution of random time intervals  $\tau$  between neighboring pulses is [28]

$$w(\tau) = H(\tau - \tau_0)p e^{-p(\tau-\tau_0)}, \quad (29)$$

where  $H(x)$  is the Heaviside step function.

In the limit  $\tau_0 \rightarrow T$ , we have  $p \rightarrow \infty$  and the process becomes deterministic and periodic. In this case the PDF of time intervals between neighboring pulses is  $w(\tau) = \delta(\tau - \tau_0)$ . When  $\tau_0 = 0$ , the stochastic process  $\eta(t)$  coincides with the white Poisson noise. The degree of periodicity, which depends on the dead time and mean period of the pulse noise, is given by  $\varrho = \tau_0/T$  and ranges from 0 to 1.

In accordance with [28], the spectral density for the pulse process under study at  $\omega = 0$  is

$$S_{\eta-\langle \eta \rangle}(0) = \frac{2f_0^2\sigma_\tau^2}{T^3}. \quad (30)$$

### 2. Pulse process with fixed time intervals

We consider periodically spaced points on a time axis with period  $T$ . The  $i$ th pulse of the FTI process is observed at  $t_i = iT + v_i$ . The time shift  $v_i$  of each pulse relative to fixed (periodic) time moments is a random quantity with zero mean value. Thus, the pulse process is characterized by the probability distribution of  $v$ .

We consider the uniform PDF of the pulse position inside an interval with length  $\tau_F \leq T$ ,

$$w(v) = \frac{1}{\tau_F}, \quad |v| \leq \frac{\tau_F}{2}. \quad (31)$$

The probability distribution of intervals  $\tau$  between two neighboring pulses is described with the following expression:

$$w(\tau) = \frac{\tau_F - |\tau - T|}{\tau_F^2}, \quad |\tau - T| \leq \tau_F. \quad (32)$$

This process can be used to present noise sources with varying degrees of randomness. The degree of periodicity can be defined as  $\varrho = 1 - \tau_F/T$ . The results of [9,29] show that  $S_{\eta-\langle \eta \rangle}(0) = 0$  for any parameter  $\varrho$ .

In practice, we usually have a set of times  $\{t_i\}$  corresponding to pulses. The two qualitatively different kinds of noise (DTDP and FTI) can be distinguished by calculating variance  $\sigma_\tau^2$  between neighboring pulses and variance  $\sigma_{N\tau}^2$  of the intervals between the  $i$ th and the  $(i + N)$ th pulses, respectively. Approximate equalities  $\sigma_\tau^2 \approx \sigma_{N\tau}^2$  and  $N\sigma_\tau^2 \approx \sigma_{N\tau}^2$  correspond to the FTI and DTDP pulse noises, respectively.

### B. Numerical simulation

First, we consider the dependence of mean value  $\langle x \rangle$  on  $D$  for different values of  $\beta$ . Figure 1 shows the results of the numerical solution of Eq. (14) with respect to  $\beta$  with fixed  $\gamma = 3/4$  and  $b = 1$ . When  $\langle x \rangle$  is independent of  $D$ , parameter  $\beta$  tends to  $\gamma + 1$  at relatively large  $a$  and small  $D$ , in accordance with Eq. (13).

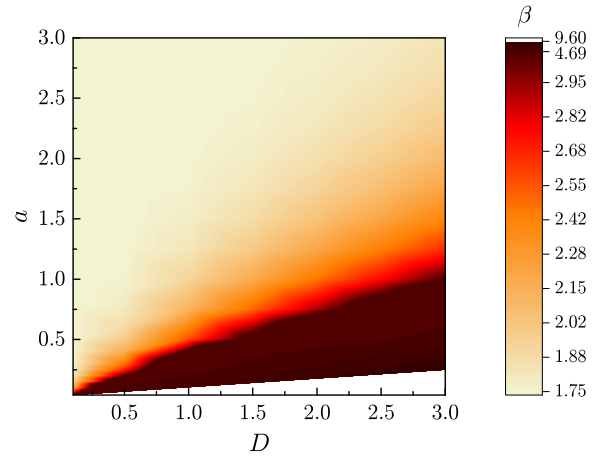


FIG. 1. Contour plot of the solution to Eq. (14) with respect to  $\beta$  vs  $a$  and  $D$  ( $\gamma = 3/4, b = 1$ ).

Figure 2 shows regions in which the mean value  $\langle x \rangle$  increases (dashed area) and decreases (blank area) with increasing  $D$ . The solid lines correspond to the solution to Eq. (14) for  $\gamma = 1/6, 1/2$ , and  $3/4$ .

We also present the results obtained by numerical integration of Eq. (1) with the DTDP noise source. The Mersenne twister [39] is used as a pseudorandom number generator. The averaging is performed over  $10^5$  numerical realizations.

Figures 3–5 show the evolution of mean value  $\langle x \rangle$  simulated with the aid of Eq. (1) at several  $\beta$  and degrees of periodicity  $\varrho = 0$  and  $0.9$ . In simulations, we use  $\gamma = 3/4, b = 1, f_0 = 0.1, T = 0.01$ , and the  $\delta$ -function initial distribution with  $x(0) = 5$ . The insets to Figs. 3–5 additionally show the results of analytical calculations obtained using expressions (13) and (16) (horizontal lines) for the same degrees of periodicity. We see that the numerical data are in good agreement with the analytical results. In particular, the numerical and analytical results almost coincide for quasiperiodic noise.

If  $\beta < \gamma + 1$ , the mean value  $\langle x \rangle$  increases with increasing  $D$  (see Fig. 3), while  $\langle x \rangle$  decreases with increasing  $D$  in the opposite case,  $\beta > \gamma + 1$  (Fig. 5). Figure 4 shows the independence of the mean value on  $D$  if  $\beta = \gamma + 1$ . Evidently,

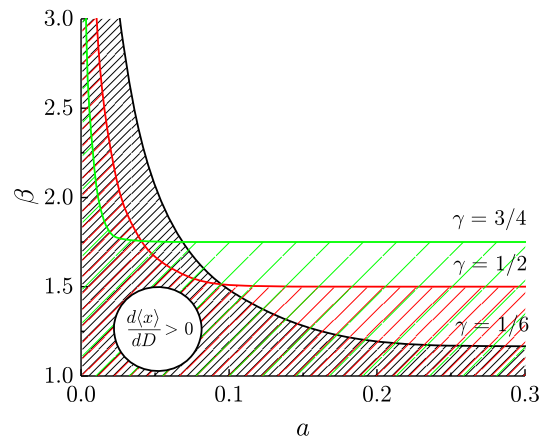


FIG. 2. Plot of the solution to Eq. (14) with respect to  $\beta$  vs  $a$  for several values of  $\gamma$  ( $b = 1, D = 0.05$ ).

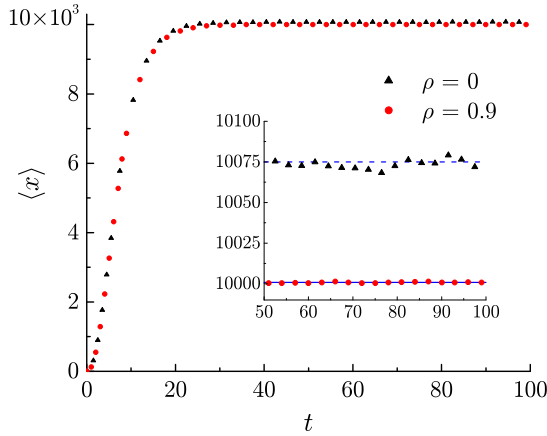


FIG. 3. Plot of mean value  $\langle x \rangle$  vs time for quasiperiodic DTDP noise ( $\rho = 0.9$ ) (circles) and totally random pulse noise ( $\rho = 0$ ) (triangles) calculated at  $\gamma = 3/4, \beta = 1, b = 1, f_0 = 0.1, T = 0.01, x(0) = 5$ . The inset additionally shows analytical solutions (13) for  $\rho = 0$  (dashed line) and 0.9 (solid line).

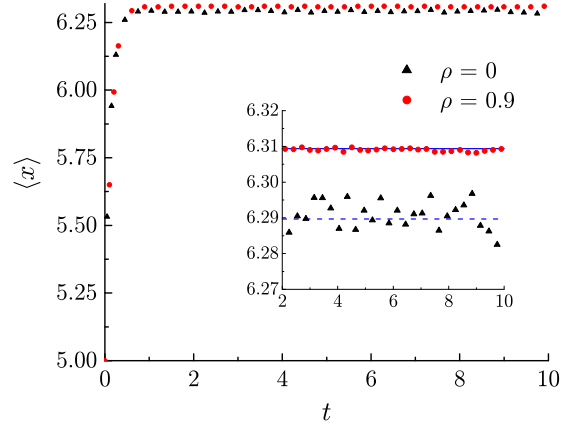


FIG. 5. Plot of mean value  $\langle x \rangle$  vs time for quasiperiodic DTDP noise ( $\rho = 0.9$ ) (circles) and totally random pulse noise ( $\rho = 0$ ) (triangles) calculated at  $\gamma = 3/4, \beta = 2, b = 1, f_0 = 0.1, T = 0.01, x(0) = 5$ . The inset additionally shows analytical solutions (13) for  $\rho = 0$  (dashed line) and 0.9 (solid line).

these statements are valid only for  $\kappa_D \gg 1$ , which is true for the parameters of Figs. 3–5.

For clarity, we summarize the above results in Fig. 6, which shows the dependence of the reduced mean value  $\langle x \rangle^* = (b/a)^{\frac{1}{\beta-\gamma}} \langle x \rangle$  on parameter  $D$  derived from Eqs. (13) and (6). The values of the parameters are  $\gamma = 3/4, a = 10$ , and  $b = 1$ . When  $D$  is about 10,  $\kappa_D < 10$  for the given parameters and formula (13) is not valid.

Note that if  $\beta > \gamma + 1$ , the mean value has at least one minimum with respect to  $D$  since its first derivative is a continuous function, which is negative for  $D \rightarrow 0$  and positive for  $D \rightarrow \infty$ .

Next, we present results obtained by numerical integration of Eq. (1), where the noise source is the FTI process of Eq. (28). Parameter  $D$  tends to zero regardless of the variance of the intervals between neighboring pulses for this noise. Thus, the

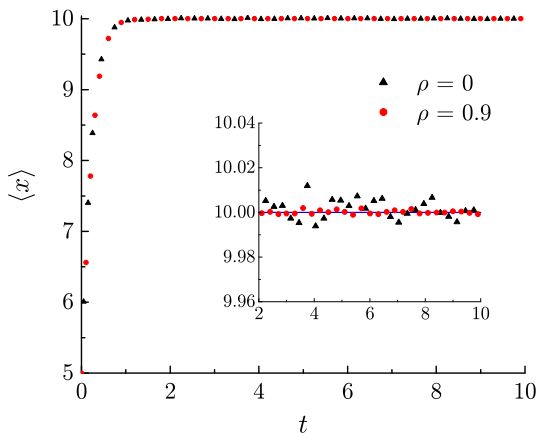


FIG. 4. Plot of mean value  $\langle x \rangle$  vs time for quasiperiodic DTDP noise ( $\rho = 0.9$ ) (circles) and totally random pulse noise ( $\rho = 0$ ) (triangles) calculated at  $\gamma = 3/4, \beta = 7/4, b = 1, f_0 = 0.1, T = 0.01, x(0) = 5$ . The inset additionally shows analytical solution (13) (solid line).

mean value  $\langle x \rangle$  also does not depend on parameter  $\rho$ . Figures 7 and 8 prove this statement.

IV. APPLICATIONS

Below, we present several examples in which the parameters of the proposed model are considered as parameters of real systems.

A. Evolution of billiardlike systems

The motion of a small particle in a quasigas of relatively large particles can be simulated using mathematical billiards. The billiard is a system in which noninteracting point particles are involved in elastic collisions with scatterers [40–42]. When scatterer boundaries are moving, the mean velocity of the particle in the scattering billiard increases. Such a phenomenon is known as the Fermi acceleration. In terms of the model [Eq. (1)], quantity  $x$  is the velocity of particle, the first term corresponds to the friction force, and random pulses in the

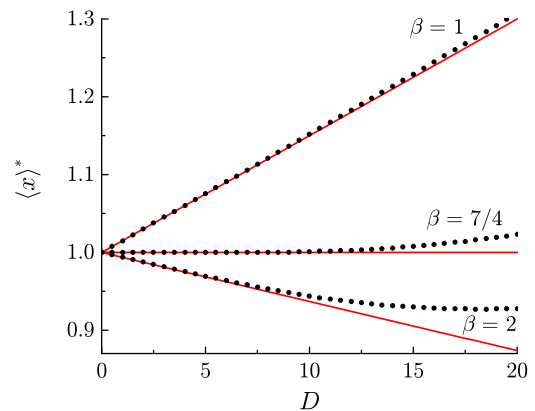


FIG. 6. Plot of the reduced mean value  $\langle x \rangle^*$  vs  $D$  for three values of  $\beta$  at  $\gamma = 3/4, a = 10$ , and  $b = 1$ : analytical solutions (13) (solid lines) and results calculated using expression (6) (dots).



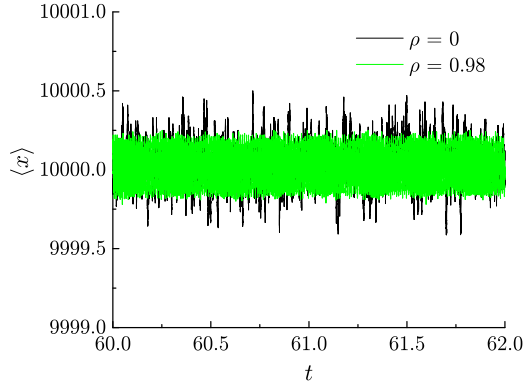


FIG. 7. Plot of the mean value  $\langle x \rangle$  vs time for two values of  $\varrho$ : quasiperiodic FTI noise ( $\varrho = 0.98$ ) [green (light gray) line] and FTI noise with maximal dispersion ( $\varrho = 0$ ) (black line). The parameters and initial condition are  $\gamma = 3/4$ ,  $\beta = 1$ ,  $b = 1$ ,  $f_0 = 0.1$ ,  $T = 0.01$ , and  $x(0) = 5$ .

second term simulate collisions with massive scatterers. The normal (constant) Fermi acceleration corresponds to  $\gamma = 1/2$ .

The billiardlike systems can be used to analyze fundamental problems of nonequilibrium thermodynamics [1–4]. The external influence on a thermodynamic system is divided into work and heat, in accordance with the first law of thermodynamics. However, such division is a complicated task and the model makes it possible to determine work and heat contributions. Correlation properties of the external force [in particular  $S(0)$ ] can be used in the analysis.

The accelerating force can be simulated as interaction with a hot thermostat characterized by the effective temperature depending on the periodicity of the force. Such effective heating of the system compensates for natural dissipation. In the model, we have generalized the concept of correlated noise. The effective temperature is determined by the stochasticity parameter  $D$  rather than the intensity of the force. For example, relatively strong highly correlated external force corresponds to low effective temperature.

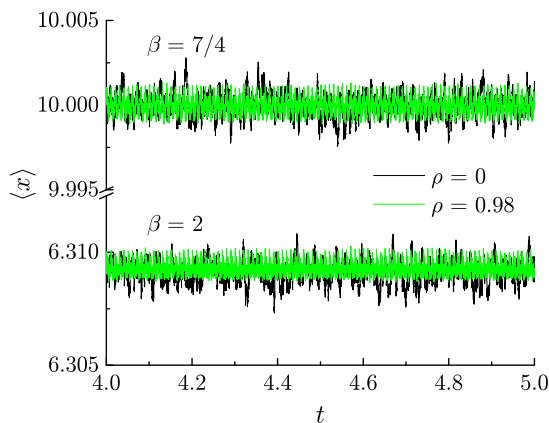


FIG. 8. Plot of the mean value  $\langle x \rangle$  vs time for two values of  $\varrho$ : quasiperiodic FTI noise ( $\varrho = 0.98$ ) [green (light gray) line] and FTI noise with maximal dispersion ( $\varrho = 0$ ) (black line). The parameters and initial condition are  $\gamma = 3/4$ ,  $b = 1$ ,  $f_0 = 0.1$ ,  $T = 0.01$ , and  $x(0) = 5$ .

## B. Diffusion of clusters on a graphite flake

The results of Refs. [43,44] show that superlubricity leads to thermal motion of graphite flakes with sizes ranging from 10 to 100  $\mu\text{m}$ . The flake motion is a sequence of jumps at random moments. A metal cluster deposited on a surface of a flake moves randomly under the influence of such jumps [5–7,45]. The cluster is accelerated by the flake and decelerated by friction. In terms of Eq. (1), quantity  $x$  is the velocity of the cluster, the first term corresponds to the friction force, and random or quasiperiodic pulses in the second term simulate the flake jumps [43,44]. The model makes it possible to determine the effect of periodicity of the flake motion using the analysis of cluster velocities.

The parameters of friction force ( $b$  and  $\beta$ ) are determined by the number of defects of the flake surface and the size and mass of clusters and independent of flake motion. The simplest model of friction corresponds to  $\beta = 0$ . Flake dynamics determines the parameters of noise  $D$  and  $a$ . The intervals between pulses  $\tau$  are independent of the cluster properties and the friction force.

Variations in the temperature and size of clusters lead to variations in the mean velocity of clusters and the growth rates of cluster structures. Moreover, an inverse problem can be solved and the motion of clusters can be used to visualize flake motion.

## C. Nonlinear filtering of a quasiperiodic electric signal

Equation (1) can be used to describe a nonlinear filter with a random input electric signal  $\eta(t)$  [8–11]. Quantity  $x$  in Eq. (1) is the output signal. Nonlinear dissipation  $-bx^\beta$  is considered.

For example, a combination of Johnson noise and Schottky noise, which originates from discrete nature of electric charge, can be considered as the input signal [46–51]. Such a combination can be a DTDP process due to anticorrelation of the motion of single electrons, acting on each other due to the Coulomb force. For an initially periodic input signal that loses periodicity, the model of FTI noise can be used.

The fact that the output signal is independent of parameter  $D$  under condition  $\beta = \gamma + 1$  (Fig. 4), the strong dependence of the output signal on the degree of periodicity (Figs. 3 and 5), and the nontrivial dependence of the mean value of the output signal on parameter  $D$  (Fig. 6) can be used to develop filters and measuring equipment.

## D. Dynamics of active Brownian particles

Active Brownian particles are assumed to have an internal propulsion mechanism (motor), which may use energy from an external source and transform it under nonequilibrium conditions into directed accelerated motion [52]. Such particles can be used to model living species or technical objects. Based on the description of individual motion of pointlike active particles by stochastic differential equations, this branch of physics considers different velocity-dependent friction functions, the impact of various types of fluctuations, and it calculates characteristic observables such as stationary velocity distributions. The apparent randomness of the dynamics of active Brownian particles may have different origins, e.g., environmental factors or internal fluctuations due to the intrinsic stochasticity of

the processes driving individual motion. For animals, the randomness may also originate from decision processes that govern the speed of individual motion and may seem random to an observer. A simple way to take into consideration such fluctuations without being able to resolve the underlying mechanisms is to introduce stochastic forces into the equations of motion of individual units.

For example, Eq. (1) can be used to describe the velocity of the flap-glide flight of birds [12–17]. Birds use intermittent flight to reduce the power cost. Over a relatively long interval of extended-wing gliding, friction force can be represented as  $-bx^\beta$ . Acceleration is reached at short intervals (pulses) of flapping. The efficiency of the flapping pulses depends on the speed, and the DTDP periodicity of the pulses provides optimal speed. The relationship of the mean velocity, the mean period, and the periodicity of flapping makes it possible to characterize the health of the bird or atmospheric convection.

### E. Population dynamics of predators

The application of stochastic methods in the analysis of population dynamics is based predominately on the equations with multiplicative noise [53–55]. Animal populations depend on randomly changing environmental conditions. For example, the number density of predators  $x$  in Eq. (1) is a result of a balance of a deterministic decrease (first term) and a random quasiperiodic increase (second term).

Strong intraspecies competition corresponds to  $\beta = 2$ , and the absence of the competition corresponds to  $\beta = 1$ . For fish and insects, parameter  $\gamma$  tends to zero, since the birth rate is almost independent of the number of adults. For mammals, an increase in population is determined by the number of adult animals, and the parameter  $\gamma$  tends to unity.

For a broader class of environmental actions in population dynamics such as pollution, disasters, rainfall, etc., it is preferable to use pulse noise that arises from the discrete origin of the events [56]. Some of these factors can be quasiperiodic. For example, noise periodicity in predator population analysis results from the periodicity of the prey population, e.g., lemmings [18–21]. Two concepts are used to describe variations in the lemming population. The first concept is based on an analysis of sun activity. In the framework of the second approach, an increase in the lemming population leads to insufficiency of food and an increase in the population of predators. The FTI and DTDP processes correspond to the first and second concepts, respectively. The problem is that we have results from the observation of lemmings only for an interval of 70 years (10–12 pulses in the framework of the model). An analysis of the population of predators based on the proposed model will make it possible to verify the concepts.

### F. Spread of infectious diseases

Equation (1) can be used to describe several infection diseases [22–26], e.g., influenza. In this case, variable  $x$  is the number of infected people.

With respect to the proposed model, the well-known epidemiological model of [26] corresponds to  $\gamma = \beta = 1$  and white Gaussian noise. Such a model does not take into

account environmental factors, life style, and traditions. The generalized Eq. (1) describes additional factors.

Positive pulses  $\eta(t)$  correspond to fast infection spreading due to weather conditions or mass gathering events [57,58]. The FTI periodicity corresponds to seasonal celebrations and weather, and the DTDP periodicity results from immunological memory. Contacts with infected people are supplemented with additional factors (e.g., contacts with animal disease carriers), and hence the parameter is  $\gamma < 1$ . Vaccination can be simulated as the parameter  $\beta > 1$ .

### G. Aging of paints on paintings

There has been considerable recent interest in the development of methods for the study of paintings. Note that single works of art or small groups are analyzed in most works. Researchers concentrate predominantly on the features of paints that are specific to particular paintings. Universal methods for dating paintings are missing in peer-reviewed journals in spite of the availability of the results of comprehensive analysis of the aging of oil paints. FTIR microspectroscopy has been employed in [59] to study time-dependent variations in the oil media of zinc-white paint in the paint layer of 19th–20th century Russian paintings. Spectroscopic data have been obtained for 493 samples of white paints from 230 paintings from several Russian museums and private collections [60]. The calculation of analytical curves that approximate experimental results (intensity ratio of spectral bands versus time) is physically meaningless and incorrect due to the significant spread of experimental data and the absence of adequate models of the aging of paintings under unknown conditions. The simplest linear dependences contradict results on averaging that indicate significantly nonlinear (threshold) character of the dependences under study. A statistical model proposed in Ref. [27] is based on the assumption that significant variations in the measured spectroscopic parameters (i.e., intensity ratios) with time can be due to (i) the spread of original compositions of paints, and (ii) changes of storage conditions. Evidently, the approach of this work can be used for alternative analysis of the experimental data. The rate of a decrease or increase in the measured intensity ratio of characteristic spectral bands can be considered as variable  $x$  in Eq. (1). The mean value of noise  $a$  is responsible for the systematic degradation of the paint layer (e.g., due to the presence of components that are involved in chemical reactions with each other), parameter  $b$  describes the initial conservation that prevents the degradation of a paint layer related to environmental factors, and zero-mean noise simulates random variations in the storage conditions.

## V. CONCLUSION

In summary, we have studied the effect of random quasiperiodic pulse pumping on a stationary-state system with nonlinear dissipation. Pulse processes with controlled periodicity have been used in the analysis of quasistable and relaxation processes. Such processes are also convenient for simulation of stationary processes in various systems. Most processes that describe random external action in applied problems can be divided into two groups. The processes of the first group are renewal processes that are characterized only by intervals

between neighboring pulses. The variance of such a process increases with time, and the correlation time increases and the stochasticity parameter decreases with increasing periodicity. DTDP is a convenient model for such processes. The processes of the second group exhibit deterministic periodicity. The variance of such processes remains constant, the correlation time is infinite, and the stochasticity parameter is zero at any periodicity. Thus, the periodicity of the FTI process does not affect statistical moments.

We have revealed the nontrivial dependence of the mean value of the main variable on stochasticity and parameters that characterize nonlinearity of pumping and dissipation. A monotonic increase in the mean value with increasing stochasticity parameter  $D$  was evident in the previous study of the stability, relaxation, and quasistable dynamics. In fact, relatively high stochasticity of noise leads to an increase in the variance of variable  $x$  and, hence, relatively large instant values of  $x$  and amplification of pumping due to multiplicative noise. A distinctive feature of the stationary state lies in the fact that the balance of both pumping and dissipation depends nonlinearly on the instant value of  $x$ . Note that the stationary state is reached only when the dissipation exponent  $\beta$  is greater than the noise multiplicativity exponent  $\gamma$ . A nontrivial decrease in the mean value with an increase in

stochasticity parameter  $D$  is observed when the dissipation exponent is greater than the noise multiplicativity exponent, at least by unity. The existence of a minimum is due to the dominant contribution of dissipation at relatively small  $D$  (viz.,  $D \ll \frac{1}{1-\gamma} [\lambda a^\lambda / b]^{1/(\lambda-1)}$ ). Parameter  $D$  corresponding to the minimum mean value can be determined analytically for a certain domain of remaining parameters. The numerical simulation shows that the results can be generalized on systems with pulse noise with controlled periodicity.

The results can be generalized on a system with a variable that decreases deterministically and increases randomly. By way of an example, we have considered the velocity of a billiard particle, the velocity of a metal cluster on a graphite flake, the output voltage of a nonlinear filter, the velocity of a flap-glide flight of birds, the number of animals in a population, the number of infected people, and the aging rate of paint on paintings.

**ACKNOWLEDGMENTS**

We are grateful to Alexander Dubkov and Ekaterina Anashkina for fruitful discussions. This work was supported by the Supercomputing Center of Lomonosov Moscow State University.

**APPENDIX A: CALCULATION OF INTEGRAL  $\int_0^\infty z^\nu e^{\frac{az}{D}} - \frac{b}{D\lambda}(1-\gamma)^{\lambda-1} z^\lambda dz$**

We consider the integral

$$\mathcal{I}_\nu = \int_0^\infty z^\nu e^{\frac{az}{D} - \frac{b}{D\lambda}(1-\gamma)^{\lambda-1} z^\lambda} dz, \text{Re} \nu > -1. \tag{A1}$$

An expansion of the function  $e^{\frac{az}{D}}$  in the Taylor series around zero and integration using [61] yields

$$\begin{aligned} \mathcal{I}_\nu &= \frac{1}{\lambda} \left( \frac{b}{D\lambda} (1-\gamma)^{\lambda-1} \right)^{-\frac{1+\nu}{\lambda}} \sum_{n=0}^\infty \frac{1}{n!} \left( \frac{a}{D} \right)^n \left( \frac{b}{D\lambda} (1-\gamma)^{\lambda-1} \right)^{-\frac{n}{\lambda}} \Gamma\left(\frac{1+\nu+n}{\lambda}\right) \\ &= \frac{1}{\lambda} \left( \frac{b}{D\lambda} (1-\gamma)^{\lambda-1} \right)^{-\frac{1+\nu}{\lambda}} {}_1\Psi_0 \left[ \left( \frac{1+\nu}{\lambda}, \frac{1}{\lambda} \right) \middle| \frac{a}{D(1-\gamma)} \left( \frac{b}{D\lambda(1-\gamma)} \right)^{-\frac{1}{\lambda}} \right], \end{aligned} \tag{A2}$$

where  ${}_p\Psi_q(\dots|z)$  is the generalized hypergeometric Wright function [31].

**APPENDIX B: CALCULATION OF INTEGRAL  $\int_0^\infty e^{i\omega[(1-\gamma)z]^{\frac{1}{1-\gamma}}} e^{\frac{az}{D} - \frac{b}{D\lambda}(1-\gamma)^{\lambda-1} z^\lambda} dz$**

We consider the integral

$$\mathcal{I}(\omega) = \int_0^\infty e^{i\omega[(1-\gamma)z]^{\frac{1}{1-\gamma}}} e^{\frac{az}{D} - \frac{b}{D\lambda}(1-\gamma)^{\lambda-1} z^\lambda} dz. \tag{B1}$$

Expanding two exponential functions in the Taylor series around zero and changing order of summation and integration, we get

$$\begin{aligned} \mathcal{I}(\omega) &= \sum_{n=0}^\infty \frac{1}{n!} \left( \frac{a}{D} \right)^n \sum_{m=0}^\infty \frac{1}{m!} (i\omega(1-\gamma)^{\frac{1}{1-\gamma}})^m \int_0^\infty z^{n+\frac{m}{1-\gamma}} e^{-\frac{b}{D\lambda}(1-\gamma)^{\lambda-1} z^\lambda} dz \\ &= \frac{1}{\lambda} \left( \frac{b}{D\lambda} (1-\gamma)^{\lambda-1} \right)^{-\frac{1}{\lambda}} \sum_{n=0}^\infty \sum_{m=0}^\infty \frac{1}{n!} \frac{1}{m!} \left[ \frac{a}{D(1-\gamma)} \left( \frac{b}{D\lambda(1-\gamma)} \right)^{-\frac{1}{\lambda}} \right]^n \left[ i\omega \left( \frac{b}{D\lambda(1-\gamma)} \right)^{-\frac{1}{\lambda(1-\gamma)}} \right]^m \Gamma\left(\frac{1+n+\frac{m}{1-\gamma}}{\lambda}\right) \\ &= \frac{1}{\lambda} \left( \frac{b}{D\lambda} (1-\gamma)^{\lambda-1} \right)^{-\frac{1}{\lambda}} H_{1,0:0,1;0,1}^{0,1:1,0;1,0} \left( \left( 1 - \frac{1}{\lambda}, \frac{1}{\lambda}, \frac{1}{\lambda(1-\gamma)} \right) : \text{---}; \text{---} \middle| \frac{-\frac{a}{D(1-\gamma)} \left( \frac{b}{D\lambda(1-\gamma)} \right)^{-\frac{1}{\lambda}}}{-i\omega \left( \frac{b}{D\lambda(1-\gamma)} \right)^{-\frac{1}{\lambda(1-\gamma)}}} \right), \end{aligned} \tag{B2}$$

where  $H_{p,q:\dots}^{0,n:\dots}(\dots|z_1, z_2)$  is the generalized hypergeometric  $H$ -function of two variables [34].



- [1] U. Seifert, *Eur. Phys. J. B* **64**, 423 (2008).
- [2] U. Seifert, *Rep. Prog. Phys.* **75**, 126001 (2012).
- [3] A.-C. Barato and U. Seifert, *Phys. Rev. Lett.* **112**, 090601 (2014).
- [4] T. Sagawa and M. Ueda, *Phys. Rev. Lett.* **109**, 180602 (2012).
- [5] P. Jensen and B. Niemeyer, *Surf. Sci.* **384**, L823 (1997).
- [6] T. Michely and J. Krug, *Islands, Mounds and Atoms* (Springer-Verlag, Berlin, 2004).
- [7] A. Perez, P. Melinon, V. Dupuis, L. Bardotti, B. Masenelli, F. Tournus, B. Prevel, J. Tuaille-Combes, E. Bernstein, A. Tamion, N. Blanc, D. Tainoff, O. Boisron, G. Guiraud, M. Broyer, M. Pellarin, N. Fatti, F. Vallee, E. Cottancin, J. Lerme, J.-L. Vialle, C. Bonnet, P. Maioli, A. Crut, C. Clavier, J. Rousset, and F. Morfin, *Int. J. Nanotech.* **7**, 523 (2010).
- [8] R. L. Stratonovich, *Topics in the Theory of Random Noise* (Gordon and Breach, New York, 1967).
- [9] B. R. Levin, *Theoretical Principles of Statistical Radiophysics* (Radio and Communications, Moscow, 1989) (in Russian).
- [10] A. V. Klyuev, A. V. Yakimov, and I. S. Zhukova, *Fluct. Noise Lett.* **14**, 1550029 (2015).
- [11] G. E. Kolosov and R. L. Stratonovich, *Automat. Remote Control* **25**, 1483 (1964).
- [12] B. W. Tobalske, *J. Exp. Biol.* **210**, 3135 (2007).
- [13] B. W. Tobalske and K. P. Dial, *J. Exp. Biol.* **187**, 1 (1994).
- [14] C. J. Pennycuik, *J. Exp. Biol.* **150**, 171 (1990).
- [15] H. Weimerskirch, J. Martin, Y. Clerquin, P. Alexandre, and S. Jiraskova, *Nature (London)* **413**, 697 (2001).
- [16] D. Lentink, U. K. Müller, E. J. Stambhuis, R. de Kat, W. van Gestel, L. L. M. Veldhuis, P. Henningsson, A. Hedenström, J. J. Videler, and J. L. van Leeuwen, *Nature (London)* **446**, 1082 (2007).
- [17] F. T. Muijres, P. Henningsson, M. Stuijvera, and A. Hedenström, *J. Theor. Biol.* **306**, 120 (2012).
- [18] N. C. Stenseth and R. A. Ims, Population Dynamics of Lemmings: Temporal and Spatial Variation — an Introduction, in *The Biology of Lemmings*, edited by N. C. Stenseth and R. A. Ims (Academic, London, 1993), pp. 61–96.
- [19] E. I. Anashkina, O. A. Chichigina, D. Valenti, A. V. Kargovsky, and B. Spagnolo, *Int. J. Mod. Phys. B* **30**, 1541003 (2016).
- [20] O. A. Chichigina, *Eur. Phys. J. B* **65**, 347 (2008).
- [21] A. Angerbjörn, M. Tannerfeldt, and S. Erlinge, *J. Anim. Ecol.* **68**, 34 (1999).
- [22] O. Chichigina, D. Valenti, and B. Spagnolo, *Fluct. Noise Lett.* **5**, L243 (2005).
- [23] Y. Wang, J. Cao, G.-Q. Sun, and J. Li, *Physica A* **412**, 137 (2014).
- [24] E. Tornatore, P. Vetro, and S. M. Buccellato, *Neural Comp. Appl.* **24**, 309 (2014).
- [25] F. Wang, X. Wang, S. Zhang, and C. Ding, *Chaos Solitons Fractals* **66**, 127 (2014).
- [26] H. Fuks, A. T. Lawniczak, and R. Duchesne, *Eur. Phys. J. B* **50**, 209 (2006).
- [27] I. A. Balakhnina, N. N. Brandt, D. Valenti, I. A. Grigorieva, B. Spagnolo, and A. Y. Chikishev, *J. Appl. Spectrosc.* **84**, 484 (2017).
- [28] O. A. Chichigina, A. A. Dubkov, D. Valenti, and B. Spagnolo, *Phys. Rev. E* **84**, 021134 (2011).
- [29] A. V. Kargovsky, O. A. Chichigina, E. I. Anashkina, D. Valenti, and B. Spagnolo, *Phys. Rev. E* **92**, 042140 (2015).
- [30] A. Dubkov and B. Spagnolo, *Acta Phys. Pol. B* **38**, 1745 (2007).
- [31] E. M. Wright, *J. London Math. Soc.* **s1-10**, 286 (1935).
- [32] A. R. Miller and I. S. Moskowitz, *Comp. Math. Appl.* **30**, 73 (1995).
- [33] A. Erdélyi, W. Magnus, F. Oberhettinger, and F. G. Tricomi, *Higher Transcendental Functions* (McGraw-Hill, New York, 1953).
- [34] A. M. Mathai, R. K. Saxena, and H. J. Haubold, *The H-Function: Theory and Applications* (Springer, New York, 2010).
- [35] A. Kilbas, R. K. Saxena, and J. Trujillo, *Fract. Calc. Appl. Anal.* **9**, 109 (2006).
- [36] R. B. Paris, *J. Comp. Appl. Math.* **234**, 488 (2010).
- [37] S. A. Akhmanov, Y. Y. Dyakov, and A. S. Chirkin, *Introduction to Statistical Radiophysics and Optics* (Springer, Berlin, 1988).
- [38] J. W. Müller, *Nucl. Instrum. Methods* **117**, 401 (1974).
- [39] M. Matsumoto and T. Nishimura, *ACM Trans. Model. Comput. Simul.* **8**, 3 (1998).
- [40] A. Y. Loskutov, A. B. Ryabov, and L. G. Akinshin, *J. Exp. Theor. Phys.* **89**, 966 (1999).
- [41] A. V. Kargovsky, E. I. Anashkina, O. A. Chichigina, and A. K. Krasnova, *Phys. Rev. E* **87**, 042133 (2013).
- [42] D. Valenti, O. A. Chichigina, A. A. Dubkov, and B. Spagnolo, *J. Stat. Mech.* (2015) P02012.
- [43] I. V. Lebedeva, A. A. Knizhnik, A. M. Popov, O. V. Ershova, Y. E. Lozovik, and B. V. Potapkin, *Phys. Rev. B* **82**, 155460 (2010).
- [44] M. M. van Wijk, M. Dienwiebel, J. W. M. Frenken, and A. Fasolino, *Phys. Rev. B* **88**, 235423 (2013).
- [45] A. Krasnova and O. Chichigina, *Moscow Univ. Phys. Bull.* **67**, 48 (2012).
- [46] W. Schottky, *Ann. Phys.* **362**, 541 (1918).
- [47] H. Birk, M. J. M. de Jong, and C. Schönenberger, *Phys. Rev. Lett.* **75**, 1610 (1995).
- [48] A. van der Ziel, *Noise in Solid State Devices and Circuits* (Wiley, New York, 1986).
- [49] C. Dekker, A. J. Scholten, F. Liefink, R. Eppenga, H. van Houten, and C. T. Foxon, *Phys. Rev. Lett.* **66**, 2148 (1991).
- [50] Y. M. Blanter and M. Büttiker, *Phys. Rep.* **336**, 1 (2000).
- [51] A. H. Steinbach, J. M. Martinis, and M. H. Devoret, *Phys. Rev. Lett.* **76**, 3806 (1996).
- [52] P. Romanczuk, M. Bär, W. Ebeling, B. Lindner, and L. Schimansky-Geier, *Eur. Phys. J. Spec. Top.* **202**, 1 (2012).
- [53] P. Barrera, S. Ciuchi, and B. Spagnolo, *J. Phys. A* **26**, L559 (1993).
- [54] S. Ciuchi, F. de Pasquale, and B. Spagnolo, *Phys. Rev. E* **47**, 3915 (1993).
- [55] S. Ciuchi, F. de Pasquale, and B. Spagnolo, *Phys. Rev. E* **54**, 706 (1996).
- [56] Y. Wu and W. Q. Zhu, *Phys. Rev. E* **77**, 041911 (2008).
- [57] P. Shi, P. Keskinocak, J. L. Swann, and B. Y. Lee, *BMC Public Health* **10**, 778 (2010).
- [58] E. Haworth, O. Barasheed, Z. A. Memish, H. Rashid, and R. Booy, *J. R. Soc. Med.* **106**, 215 (2013).
- [59] I. A. Balakhnina, N. N. Brandt, A. Y. Chikishev, Y. I. Grenberg, I. A. Grigorieva, I. F. Kadikova, and S. A. Pisareva, *Appl. Spectrosc.* **70**, 1150 (2016).
- [60] The samples were taken from paintings of I. K. Aivazovsky, A. K. Savrasov, K. E. Makovsky, P. P. Konchalovsky, M. F. Larionov, W. W. Kandinsky, N. I. Altman, K. S. Malevich, Z. Y. Serebriakova, B. M. Kustodieva, A. M. Rodchenko, R. R. Falk, A. V. Lentulov, and I. E. Grabar.
- [61] I. S. Gradshteyn and I. M. Ryzhik, *Table of Integrals, Series, and Products* (Elsevier/Academic, Amsterdam, 2007).